Chapter 5

Spectral FE Analysis with Magnetostrictive Patches

5.1 Introduction

As mentioned earlier, determination of smaller cracks requires signals having high frequency content. That is, the problem translates itself to a wave propagation problem, wherein, in addition to phase information of the response being important, higher order modes participate in the response. For such problem, FEM requires enormous mesh sizes. This problem can be alleviated little using superconvergent elements. The best way to handle such situation is to formulate elements in the frequency domain. Spectral FE is one such formulation that will be addressed in this chapter.

Wave propagation in a structure is caused by high frequency impact loading. When such loading is applied to a structure, it will force all the higher-order modes to participate in the response. At high frequencies, the wavelength is small and for an accurate prediction by the finite element (FE) method, the element length should be one fourth to one sixth of the wavelength [196]. Hence, FE analysis of wave propagation incurs heavy computational costs. The spectral element method (SEM) is arguably the best alternative for such problems [108]. The method is based upon the domain transfer method. Here, the governing equation is transformed first into the frequency domain using a discrete Fourier transform (DFT). In doing so, for 1-D waveguides, the governing partial differential equation (PDE) is reduced to a set of ordinary differential equations (ODE) with constant coefficients, where the time coordinate gives way to the frequency, which is introduced as a parameter. The resulting ODEs can be solved exactly. The elements are formulated using the exact solution of the governing ODEs as an interpolating function. The use of the exact solution results in an exact mass distribution and thus in an exact dynamic stiffness matrix. Hence, in absence of any discontinuity or irregularity in geometry, one element is sufficient to handle a beam of any length. This feature substantially reduces the size of the global dynamic stiffness matrix to be inverted and the problem (matrix) size is many orders smaller than the sizes involved in conventional FEM. The steps to be followed in SEM are as follows: First, the input forcing function is fed into Fast Fourier Transform (FFT) program, which will split the forcing history into frequencies, and the real and imaginary parts of the force history. These frequencies are real, and element dynamic stiffness matrix is generated at each frequency. These are assembled and solved as in conventional FEM. After assembly, the structure is solved for unit impulse; which will directly give Frequency Response Function (FRF). The FRF is then convolved with load to get the required response. Finally, inverse fast Fourier transform (IFFT) is used to get the time history of the response. In addition to the smaller system sizes, there are many advantages inherent to the SEM. These are summarized below:

1. A compact matrix formulation is available, which can accommodate any number of nodal variables in a spectral finite element model (SFEM) and hence suitable for automation. It is stiffness formulated. This means the process of assemblage for complex structures is easy.

2. The mass distribution is modelled exactly and hence only one element is sufficient to describe a whole beam without the need for subdivisions. This makes the resulting system of dynamic equations very small and hence computationally efficient.

3. The problem to be solved is repeated many times in data-independent manner. This inherent parallelism of the spectral approach can be utilized on multiprocessor machines.

4. The FRF is the direct by-product of the approach.

5. Since the system transfer function is direct by product of the approach, performing inverse problems, such as, system identification or the force identification, is also straightforward.

6. Infinite domain can be easily modelled by just leaving out the terms containing the reflected coefficients from the exact solution. Such a single edge non-resonant elements are called the throw-off element. When added to the structure, it amounts to adding maximum damping for the structure.

7. The classical static stiffness matrix can be obtained from the spectral stiffness matrix in a zero-frequency limit.

8. Responses can be viewed both in time and frequency domain in a single analysis. The frequency domain information such as transfer functions and system functions are generated automatically.

9. The method is easily amenable for control related problems. A novel active spectral element (see [246]) is formulated for this purpose. This has great utility in smart structure research for noise and vibration suppression.

10. As opposed to using modal analysis, in the SFEM is based on computation of wavenumbers and frequency domain fields (displacements, strains, stresses etc.) i.e. the spectral amplitudes, at each frequency sampling points in FFT. The consideration of frequency bandwidth is not limited by the choice of the finite element discretization, i.e. even a single Spectral Element can be used for a uniform beam excited by high frequency loads. Also, the time history of the applied load can be arbitrary.

11. Cut-off frequency is one parameter that determines the need for higher order beam theory. In elementary beams, the cut-off frequency is at infinity i.e. shear mode appears as evanescent mode, which never propagates. If the frequency of interest is within the occurrence of the cut-off frequency, then the elementary beam theory is sufficient to predict the response. In FSDT the shear mode, which is evanescent to start with, begins to propagate beyond cut-off frequency. This aspect will be dwelt in greater detail in this chapter.

5.1.1 Existing Literature

Spectral elements for an elementary rod [109], elementary beam [110], [111], elementary composite beam [249], composite tube [250], and a 2-D membrane element [330] are reported in literature.

Several higher-order spectral elements for isotropic and anisotropic one-dimensional wave guides are available in the literature. Spectral elements are developed for the isotropic Mindlin Herman rod [256], the isotropic Timoshenko beam [140] and the composite Timoshenko beam [248].

Introducing Poisson's contraction and its higher order gradients in the displacement field give rise to additional propagating modes at high frequencies. In addition, the longitudinal wave in the structure becomes dispersive. Conventional Higher order Shear Deformation Theory (HSDT) allows no depth wise variation of transverse displacement. Further, the displacement field with lateral contraction predicts nonzero normal stress, which is altogether neglected in HSDT. Hence, for a deep beam and high frequency loading, HSDT will not predict the accurate dynamic response of the structure. An exact FE was developed for isotropic materials by Gopalakrishnan [139], which takes Poisson's contraction into account. More recently, an exact FE is developed for a composite beam with Poisson's contraction [64]. Extensive study on wave propagation in anisotropic and inhomogeneous structure is done by Chakraborty in reference [59]. In this study, he has shown that the dispersiveness of an axial mode is due to the presence of lateral contraction. In recent study, Batra and Aimmanee [31] used finite element mixed formulation to satisfy traction boundary conditions on the top and the bottom surfaces with higher order shear and normal deformable plate theories.

In this chapter, a new higher order spectral element is developed for wave propagation analysis of a magnetostrictive embedded composite beam in the presence of thermal, magnetic and mechanical loading. The element is based on the coupled formulation of Higher order Shear deformation with higher order Poisson contraction Theory (HSPT). The HSDT is enhanced through the introduction of higher number of lateral contractional mode. Numerical examples are directed towards highlighting the effect of the requirement of higher order theories on the structural and magnetic responses. The spectrum and the dispersion relations are studied in detail. Response of structure for high frequency modulated pulse with different order of beam assumption is outlined and shown the error in lower order models. Magnetostrictive sensor open circuit voltages due to broadband force excitation are computed. Finally, as a demonstration of its capability to handle inverse problems, applied broadband force history in a cantilever composite beam is reconstructed from the response of magnetostrictive sensor open circuit voltage history, using deconvolution property of the spectral formulation.

This chapter is organized as follows. First the variational formulation is illustrated to obtain the governing differential equations of Higher order Shear deformable and Poisson contractible (HSPT) beam. Subsequently, we derive spectral solution for these governing equations and formulate the spectral finite element of the beam element with embedded magnetostrictive patches. In Section-5.4, several examples are considered for the verification of the element, demonstration of the importance of higher order theories, propagation of the extra shear and contraction modes, alteration in group speed due to the presence of higher order degrees of freedom. Finally, in Subsection-5.4.2, force identification is demonstrated from magnetostrictive sensor response.

5.2 FE Formulation of an n^{th} Order Shear Deformable Beam with n^{th} Order Poisson's Contraction

Considering the Un^{th} order shear deformation theory along with Wn^{th} order Poisson's contraction effects, the axial and the transverse displacement fields can be written as

$$U(x,y,z,t) = u_0(x,t) + \sum_{i=1}^{Un} z^i u_i(x,t)\ ,\ W(x,y,z,t) = w_0(x,t) + \sum_{i=1}^{Wn} z^i w_i\ , \tag{5.1}$$

where u_0 and w_0 are axial and transverse displacements in the reference plane respectively and z is thickness coordinate measured from the reference plane. w_i are the contractional strain and their higher order in transverse direction due to the effect of the Poisson ratio. Magnetic fields are assumed as

$$H_x(x,y,z,t) = H_{xp}(x,t), \qquad H_y(x,y,z,t) = 0, \qquad H_z(x,y,z,t) = 0 \tag{5.2}$$

where H_x, H_y and H_z are the component of magnetic fields at location (x,y,z) in X, Y and Z direction respectively. H_{xp} is X directional magnetic field at mid plane of the magnetostrictive patch p. The magnetic field along the thickness direction within the particular layer is assumed as constant. Using Equation-(5.1), the linear strains can be written as

$$\begin{aligned}
\varepsilon_{xx} &= u_{0,x} + \sum_{i=1}^{Un} z^i u_{i,x} - \alpha\Delta T, \\
\varepsilon_{zz} &= \sum_{i=1}^{Wn} i z^{(i-1)} w_i - \alpha\Delta T, \\
\gamma_{xz} &= \sum_{i=1}^{Un} i z^{(i-1)} u_i(x,t) + w_{0,x} + \sum_{i=1}^{Wn} z^i w_{i,x}.
\end{aligned} \tag{5.3}$$

α is coefficient of thermal expansion of the material and ΔT is the temperature change to which the beam is subjected. The constitutive relation for material is assumed to be of the form

$$
\begin{aligned}
\left\{\begin{array}{c}\sigma_{xx}\\ \sigma_{zz}\\ \tau_{xz}\end{array}\right\} &= \left[\begin{array}{ccc}\bar{Q}_{11} & \bar{Q}_{13} & 0\\ \bar{Q}_{13} & \bar{Q}_{33} & 0\\ 0 & 0 & \bar{Q}_{55}\end{array}\right]\left\{\begin{array}{c}\varepsilon_{xx}\\ \varepsilon_{zz}\\ \gamma_{xz}\end{array}\right\} - \left\{\begin{array}{c}e_{11}\\ e_{13}\\ e_{15}\end{array}\right\} H\ ,\\
B_{xx} &= \left[\begin{array}{ccc}e_{11} & e_{13} & e_{15}\end{array}\right]\left\{\begin{array}{c}\varepsilon_{xx}\\ \varepsilon_{zz}\\ \gamma_{xz}\end{array}\right\} + \ \mu^{\epsilon}\ H\ ,
\end{aligned}
\tag{5.4}
$$

where σ_{xx} and ε_{xx}, are normal stresses and normal strains in the x direction, σ_{zz} and ε_{zz}, are normal stresses and normal strains in the z direction and τ_{xz} and γ_{xz} are shear stress and shear strain in the $x-z$ plane. $\bar{Q}_{11}(z)$, $\bar{Q}_{13}(z)$, $\bar{Q}_{33}(z)$ and $\bar{Q}_{55}(z)$ are Young's and Shear module, which are functions of depth z. The strain energy (S), magnetic energy (W_m) and kinetic energy (T) are then given by

$$
\begin{aligned}
S &= \frac{1}{2}\int_0^L \int_A (\sigma_{xx}\varepsilon_{xx} + \sigma_{zz}\varepsilon_{zz} + \tau_{xz}\gamma_{xz})\, dA\, dx\ ,\\
W_m &= \int_0^L \int_A (\frac{1}{2}B_{xx}H + In\mu^{\sigma}H)\, dA\, dx\ ,\\
T &= \frac{1}{2}\int_0^L \int_A \varrho(z)(\dot{U}^2 + \dot{W}^2)\, dA\, dx\ ,
\end{aligned}
\tag{5.5}
$$

where $(\dot{})$ denotes the time derivative. Here $\varrho(z)$, L and A are the density, the length and the area of cross-section of the beam, respectively. Applying Hamilton's principle, the following differential equations of motion are obtained in terms of the mechanical degrees of freedom (u_0, w_0, w_i and u_i) and magnetic degrees of freedom H :

$$
\begin{aligned}
\partial u_0 : \quad & I_0\ddot{u}_0 + \sum_{i=1}^{Un} I_i\ddot{u}_i - A_{11}\frac{\partial^2 u}{\partial x^2} - \sum_{i=1}^{Un} A_{11}^{[i]}\frac{\partial^2 u_i}{\partial x^2} - \sum_{i=1}^{Wn} iA_{13}^{[i-1]}\frac{\partial w_i}{\partial x}\\
& + A_{11}^{e}\frac{\partial H}{\partial x} = 0\ ,
\end{aligned}
\tag{5.6}
$$

$$
\begin{aligned}
\partial u_m : \quad & I_{[m]}\ddot{u}_0 + \sum_{i=1}^{Un} I_{[i+m]}\ddot{u}_i - A_{11}^{[m]}\frac{\partial^2 u}{\partial x^2} - \sum_{i=1}^{Un} A_{11}^{[i+m]}\frac{\partial^2 u_i}{\partial x^2} - \sum_{i=1}^{Wn} iA_{13}^{[i+m-1]}\frac{\partial w_i}{\partial x}\\
& + mA_{55}^{[m-1]}\frac{\partial w_0}{\partial x} + \sum_{i=1}^{Wn} mA_{55}^{[i+m-1]}\frac{\partial w_i}{\partial x} + \sum_{i=1}^{Un} imA_{55}^{[i+m-2]}u_i\\
& + A_{11e}^{[m]}\frac{\partial H}{\partial x} - mA_{15e}^{[m-1]}H = 0\ ,
\end{aligned}
\tag{5.7}
$$

$$\partial w_0 : \quad I_0\ddot{w}_0 + \sum_{i=1}^{Wn} I_i\ddot{w}_i - A_{55}\frac{\partial^2 w}{\partial x^2} - \sum_{i=1}^{Un} iA_{55}^{[i-1]}\frac{\partial u_i}{\partial x} - \sum_{i=1}^{Wn} A_{55}^{[i]}\frac{\partial^2 w_i}{\partial x^2} + A_{15}^{e}\frac{\partial H}{\partial x} = 0 \ , \tag{5.8}$$

$$\begin{aligned}\partial w_m : \quad & I_{[m]}\ddot{w}_0 + \sum_{i=1}^{Wn} I_{i+m}\ddot{w}_i + mA_{13}^{[m-1]}\frac{\partial u_0}{\partial x} + m\sum_{i=1}^{Un} A_{13}^{[i+m-1]}\frac{\partial u_i}{\partial x} + \sum_{i=1}^{Wn} imA_{33}^{[i+m-2]}w_i \\ & -A_{55}^{[m]}\frac{\partial^2 w}{\partial x^2} - \sum_{i=1}^{Un} iA_{55}^{[i+m-1]}\frac{\partial u_i}{\partial x} - k_d\sum_{i=1}^{Wn} A_{55}^{[i+m]}\frac{\partial^2 w_i}{\partial x^2} \\ & -mA_{13\alpha}^{[m-1]}(\Delta T) - mA_{33\alpha}^{[m-1]}(\Delta T) - mA_{13e}^{[m-1]}H + A_{15e}^{[m]}\frac{\partial H}{\partial x} = 0 \ ,\end{aligned} \tag{5.9}$$

$$\begin{aligned}\partial H : \quad & -A_{11e}^{[0]}\frac{\partial u_0}{\partial x} - \sum_{i=1}^{Un} A_{11e}^{[i]}\frac{\partial u_i}{\partial x} - \sum_{i=1}^{Wn} iA_{13e}^{[i-1]}w_i - A_{15e}^{[0]}\frac{\partial w_0}{\partial x} - \sum_{i=1}^{Un} iA_{15e}^{[i-1]}u_i \\ & -\sum_{i=1}^{Wn} A_{15e}^{[i]}\frac{\partial w_i}{\partial x} - A_{\mu}^{\epsilon}H + InA_{\mu}^{\sigma} + (A_{11e\alpha} + A_{13e\alpha})(\Delta T) = 0 \ ,\end{aligned} \tag{5.10}$$

The associated force boundary conditions are given by

$$\begin{aligned}N_x^{[0]} &= A_{11}^{[0]}\frac{\partial u_0}{\partial x} + \sum_{i=1}^{Un} A_{11}^{[i]}\frac{\partial u_i}{\partial x} + \sum_{i=1}^{Wn} iA_{13}^{[i-1]}w_i - A_{11e}^{[0]}H + (A_{11\alpha}^{[0]} + B_{13\alpha}^{[0]})(\Delta T) \ , \\ N_x^{[m]} &= A_{11}^{[m]}\frac{\partial u_0}{\partial x} + \sum_{i=1}^{Un} A_{11}^{[i+m]}\frac{\partial u_i}{\partial x} + (A_{11\alpha}^{[m]} + B_{13\alpha}^{[m]})(\Delta T) + \sum_{i=1}^{Wn} iA_{13}^{[i+m-1]}w_i - A_{11e}^{[m]}H \ , \\ V_x^{[0]} &= A_{55}^{[0]}\frac{\partial w_0}{\partial x} + \sum_{i=1}^{Un} iA_{55}^{[i-1]}u_i + \sum_{i=1}^{Wn} A_{55}^{[i]}\frac{\partial w_i}{\partial x} - A_{15e}^{[0]}H \ , \\ V_x^{[m]} &= A_{55}^{[m]}\frac{\partial w_0}{\partial x} + \sum_{i=1}^{Un} iA_{55}^{[i+m-1]}u_i + \sum_{i=1}^{Wn} A_{55}^{[i+m]}\frac{\partial w_i}{\partial x} - A_{15e}^{[m]}H \ ,\end{aligned} \tag{5.11}$$

at two ends of the beam. Here $I_0, I_1, I_2, ...I_n$ are the mass, first moment of mass and second moment of mass ... n^{th} moment of mass per unit length of the beam. These mass moments are given by

$$[I_k] = \int_{-h/2}^{+h/2} \varrho(z)[z^k]bdz \ . \tag{5.12}$$

where the stiffness coefficients are given by

$$\left[A_{ij}^{[k]}\right] = \int_{-h/2}^{+h/2} \bar{Q}_{ij}\left[z^k\right]bdz \ , \tag{5.13}$$

The cross-sectional constant strain and constant stress permeability coefficients are written as

$$\begin{bmatrix} A_\mu^\epsilon & A_\mu^\sigma \end{bmatrix} = \int_{-h/2}^{+h/2} \begin{bmatrix} \mu^\epsilon & \mu^\sigma \end{bmatrix} bdz \;, \tag{5.14}$$

and similarly the cross-sectional magneto-mechanical and thermo-magnetic coupling stress coefficients can be written as

$$\begin{bmatrix} A_{ije}^{[k]} & A_{ije\alpha}^{[k]} \end{bmatrix} = \int_{-h/2}^{+h/2} e_{ij} z^k \begin{bmatrix} 1 & \alpha \end{bmatrix} bdz \;, \tag{5.15}$$

The cross-sectional thermal stiffness coefficients, are similarly written as

$$\left[A_{ij\alpha}^{[k]}\right] = \int_{-h/2}^{+h/2} \alpha \bar{Q}_{ij} \left[z^k\right] bdz \;, \tag{5.16}$$

Form Equation-(5.10), H can be written as

$$H = -\frac{1}{A_\mu^\epsilon}\left[A_{11e}^{[0]}\frac{\partial u_0}{\partial x} + \sum_{i=1}^{Un} A_{11e}^{[i]}\frac{\partial u_i}{\partial x} + \sum_{i=1}^{Wn} iA_{13e}^{[i-1]} w_i + A_{15e}^{[0]}\frac{\partial w_0}{\partial x} + \sum_{i=1}^{Un} iA_{15e}^{[i-1]} u_i \right.$$

$$\left. + \sum_{i=1}^{Wn} A_{15e}^{[i]}\frac{\partial w_i}{\partial x} - InA_\mu^\sigma - (A_{11e\alpha} + A_{13e\alpha})(\Delta T)\right], \tag{5.17}$$

and

$$\frac{\partial H}{\partial x} = -\frac{1}{A_\mu^\epsilon}\left[A_{11e}^{[0]}\frac{\partial^2 u}{\partial x^2} + \sum_{i=1}^{Un} A_{11e}^{[i]}\frac{\partial^2 u_i}{\partial x^2} + \sum_{i=1}^{Wn} iA_{13e}^{[i-1]}\frac{\partial w_i}{\partial x} + A_{15e}^{[0]}\frac{\partial^2 w}{\partial x^2} \right.$$

$$\left. + \sum_{i=1}^{Un} iA_{15e}^{[i-1]}\frac{\partial u_i}{\partial x} + \sum_{i=1}^{Wn} A_{15e}^{[i]}\frac{\partial^2 w_i}{\partial x^2}\right], \tag{5.18}$$

substituting H in Equations-(5.6-5.9) we get

$$\partial u_0 : I_0\ddot{u}_0 + \sum_{i=1}^{Un} I_i\ddot{u}_i - A_{11}\frac{\partial^2 u}{\partial x^2} - \sum_{i=1}^{Un} A_{11}^{[i]}\frac{\partial^2 u_i}{\partial x^2} - \sum_{i=1}^{Wn} iA_{13}^{[i-1]}\frac{\partial w_i}{\partial x} \qquad .$$

$$-\frac{A_{11}^e}{A_\mu^\epsilon}\left[A_{11e}^{[0]}\frac{\partial^2 u}{\partial x^2} + \sum_{i=1}^{Un} A_{11e}^{[i]}\frac{\partial^2 u_i}{\partial x^2} + \sum_{i=1}^{Wn} iA_{13e}^{[i-1]}\frac{\partial w_i}{\partial x} + A_{15e}^{[0]}\frac{\partial^2 w}{\partial x^2}\right.$$

$$+\sum_{i=1}^{Un} iA_{15e}^{[i-1]}\frac{\partial u_i}{\partial x}+\sum_{i=1}^{Wn} A_{15e}^{[i]}\frac{\partial^2 w_i}{\partial x^2}\Bigg]=0\ , \tag{5.19}$$

$$\partial w_0 : I_0\ddot{w}_0+\sum_{i=1}^{Wn} I_i\ddot{w}_i - A_{55}\frac{\partial^2 w}{\partial x^2}-\sum_{i=1}^{Un} iA_{55}^{[i-1]}\frac{\partial u_i}{\partial x}-\sum_{i=1}^{Wn} A_{55}^{[i]}\frac{\partial^2 w_i}{\partial x^2}$$

$$-\frac{A_{15}^{e}}{A_{\mu}^{\epsilon}}\Bigg[A_{11e}^{[0]}\frac{\partial^2 u}{\partial x^2}+\sum_{i=1}^{Un} A_{11e}^{[i]}\frac{\partial^2 u_i}{\partial x^2}+\sum_{i=1}^{Wn} iA_{13e}^{[i-1]}\frac{\partial w_i}{\partial x}+A_{15e}^{[0]}\frac{\partial^2 w}{\partial x^2}$$

$$+\sum_{i=1}^{Un} iA_{15e}^{[i-1]}\frac{\partial u_i}{\partial x}+\sum_{i=1}^{Wn} A_{15e}^{[i]}\frac{\partial^2 w_i}{\partial x^2}\Bigg]=0\ , \tag{5.20}$$

$$\partial w_m : I_{[m]}\ddot{w}_0+\sum_{i=1}^{Wn} I_{i+m}\ddot{w}_i + mA_{13}^{[m-1]}\frac{\partial u_0}{\partial x}+m\sum_{i=1}^{Un} A_{13}^{[i+m-1]}\frac{\partial u_i}{\partial x}+\sum_{i=1}^{Wn} imA_{33}^{[i+m-2]}w_i$$

$$-A_{55}^{[m]}\frac{\partial^2 w}{\partial x^2}-\sum_{i=1}^{Un} iA_{55}^{[i+m-1]}\frac{\partial u_i}{\partial x}-k_d\sum_{i=1}^{Wn} A_{55}^{[i+m]}\frac{\partial^2 w_i}{\partial x^2}$$

$$-\frac{A_{15e}^{[m]}}{A_{\mu}^{\epsilon}}\Bigg[A_{11e}^{[0]}\frac{\partial^2 u}{\partial x^2}+\sum_{i=1}^{Un} A_{11e}^{[i]}\frac{\partial^2 u_i}{\partial x^2}+\sum_{i=1}^{Wn} iA_{13e}^{[i-1]}\frac{\partial w_i}{\partial x}+A_{15e}^{[0]}\frac{\partial^2 w}{\partial x^2}$$

$$+\sum_{i=1}^{Un} iA_{15e}^{[i-1]}\frac{\partial u_i}{\partial x}+\sum_{i=1}^{Wn} A_{15e}^{[i]}\frac{\partial^2 w_i}{\partial x^2}\Bigg]$$

$$+\frac{mA_{13e}^{[m-1]}}{A_{\mu}^{\epsilon}}\Bigg[A_{11e}^{[0]}\frac{\partial u_0}{\partial x}+\sum_{i=1}^{Un} A_{11e}^{[i]}\frac{\partial u_i}{\partial x}+\sum_{i=1}^{Wn} iA_{13e}^{[i-1]}w_i+A_{15e}^{[0]}\frac{\partial w_0}{\partial x}$$

$$+\sum_{i=1}^{Un} iA_{15e}^{[i-1]}u_i+\sum_{i=1}^{Wn} A_{15e}^{[i]}\frac{\partial w_i}{\partial x}\Bigg]+V_{bT}^{[m]}+V_{bI}^{[m]}=0\ , \tag{5.21}$$

$$\partial u_m : I_{[m]}\ddot{u}_0+\sum_{i=1}^{Un} I_{[i+m]}\ddot{u}_i - A_{11}^{[m]}\frac{\partial^2 u}{\partial x^2}-\sum_{i=1}^{Un} A_{11}^{[i+m]}\frac{\partial^2 u_i}{\partial x^2}-\sum_{i=1}^{Wn} iA_{13}^{[i+m-1]}\frac{\partial w_i}{\partial x}$$

$$+mA_{55}^{[m-1]}\frac{\partial w_0}{\partial x}+\sum_{i=1}^{Wn} mA_{55}^{[i+m-1]}\frac{\partial w_i}{\partial x}+\sum_{i=1}^{Un} imA_{55}^{[i+m-2]}u_i$$

$$-\frac{A_{11e}^{[m]}}{A_\mu^\epsilon}\left[A_{11e}^{[0]}\frac{\partial^2 u}{\partial x^2}+\sum_{i=1}^{Un} A_{11e}^{[i]}\frac{\partial^2 u_i}{\partial x^2}+\sum_{i=1}^{Wn} iA_{13e}^{[i-1]}\frac{\partial w_i}{\partial x}+A_{15e}^{[0]}\frac{\partial^2 w}{\partial x^2}\right.$$

$$\left.+\sum_{i=1}^{Un} iA_{15e}^{[i-1]}\frac{\partial u_i}{\partial x}+\sum_{i=1}^{Wn} A_{15e}^{[i]}\frac{\partial^2 w_i}{\partial x^2}\right]$$

$$+\frac{mA_{15e}^{[m-1]}}{A_\mu^\epsilon}\left[A_{11e}^{[0]}\frac{\partial u_0}{\partial x}+\sum_{i=1}^{Un} A_{11e}^{[i]}\frac{\partial u_i}{\partial x}+\sum_{i=1}^{Wn} iA_{13e}^{[i-1]}w_i+A_{15e}^{[0]}\frac{\partial w_0}{\partial x}\right.$$

$$\left.+\sum_{i=1}^{Un} iA_{15e}^{[i-1]}u_i+\sum_{i=1}^{Wn} A_{15e}^{[i]}\frac{\partial w_i}{\partial x}\right]+N_{bT}^{[m]}+N_{bI}^{[m]}=0\ , \tag{5.22}$$

Similarly, boundary conditions from Equation-(5.11) can be written as

$$\begin{aligned}
N_x^{[0]} &= A_{11}^{[0]}\frac{\partial u_0}{\partial x}+\sum_{i=1}^{Un} A_{11}^{[i]}\frac{\partial u_i}{\partial x}+\sum_{i=1}^{Wn} iA_{13}^{[i-1]}w_i \\
&+ \frac{A_{11e}^{[0]}}{A_\mu^\epsilon}\left[A_{11e}^{[0]}\frac{\partial u_0}{\partial x}+\sum_{i=1}^{Un} A_{11e}^{[i]}\frac{\partial u_i}{\partial x}+\sum_{i=1}^{Wn} iA_{13e}^{[i-1]}w_i+A_{15e}^{[0]}\frac{\partial w_0}{\partial x}\right. \\
&+ \left.\sum_{i=1}^{Un} iA_{15e}^{[i-1]}u_i+\sum_{i=1}^{Wn} A_{15e}^{[i]}\frac{\partial w_i}{\partial x}\right]+N_{nT}^{[0]}+N_{nI}^{[0]}\ , \\
N_x^{[m]} &= A_{11}^{[m]}\frac{\partial u_0}{\partial x}+\sum_{i=1}^{Un} A_{11}^{[i+m]}\frac{\partial u_i}{\partial x}+\sum_{i=1}^{Wn} iA_{13}^{[i+m-1]}w_i \\
&+ \frac{A_{11e}^{[m]}}{A_\mu^\epsilon}\left[A_{11e}^{[0]}\frac{\partial u_0}{\partial x}+\sum_{i=1}^{Un} A_{11e}^{[i]}\frac{\partial u_i}{\partial x}+\sum_{i=1}^{Wn} iA_{13e}^{[i-1]}w_i+A_{15e}^{[0]}\frac{\partial w_0}{\partial x}\right.
\end{aligned}$$

$$+ \quad \sum_{i=1}^{Un} iA_{15e}^{[i-1]}u_i + \sum_{i=1}^{Wn} A_{15e}^{[i]}\frac{\partial w_i}{\partial x}\Bigg] + N_{nT}^{[m]} + N_{nI}^{[m]} \ ,$$

$$V_x^{[0]} = A_{55}^{[0]}\frac{\partial w_0}{\partial x} + \sum_{i=1}^{Un} iA_{55}^{[i-1]}u_i + \sum_{i=1}^{Wn} A_{55}^{[i]}\frac{\partial w_i}{\partial x} \qquad .$$

$$+ \quad \frac{A_{15e}^{[0]}}{A_\mu^\epsilon}\Bigg[A_{11e}^{[0]}\frac{\partial u_0}{\partial x} + \sum_{i=1}^{Un} A_{11e}^{[i]}\frac{\partial u_i}{\partial x} + \sum_{i=1}^{Wn} iA_{13e}^{[i-1]}w_i + A_{15e}^{[0]}\frac{\partial w_0}{\partial x}$$

$$+ \quad \sum_{i=1}^{Un} iA_{15e}^{[i-1]}u_i + \sum_{i=1}^{Wn} A_{15e}^{[i]}\frac{\partial w_i}{\partial x}\Bigg] + V_{nT}^{[0]} + V_{nI}^{[0]} \ ,$$

$$V_x^{[m]} = A_{55}^{[m]}\frac{\partial w_0}{\partial x} + \sum_{i=1}^{Un} iA_{55}^{[i+m-1]}u_i + \sum_{i=1}^{Wn} A_{55}^{[i+m]}\frac{\partial w_i}{\partial x}$$

$$+ \quad \frac{A_{15e}^{[m]}}{A_\mu^\epsilon}\Bigg[A_{11e}^{[0]}\frac{\partial u_0}{\partial x} + \sum_{i=1}^{Un} A_{11e}^{[i]}\frac{\partial u_i}{\partial x} + \sum_{i=1}^{Wn} iA_{13e}^{[i-1]}w_i + A_{15e}^{[0]}\frac{\partial w_0}{\partial x}$$

$$+ \quad \sum_{i=1}^{Un} iA_{15e}^{[i-1]}u_i + \sum_{i=1}^{Wn} A_{15e}^{[i]}\frac{\partial w_i}{\partial x}\Bigg] + V_{nT}^{[m]} + V_{nI}^{[m]} \ , \tag{5.23}$$

Where $N_{bI}^{[m]}, V_{bI}^{[m]}, N_{nI}^{[0]}, N_{nI}^{[m]}, V_{nI}^{[m]}, V_{nI}^{[0]}$, $N_{bT}^{[m]}, V_{bT}^{[m]}, N_{nT}^{[0]}, N_{nT}^{[m]}, V_{nT}^{[m]}, V_{nT}^{[0]}$ are given by

$$V_{bI}^{[m]} = -\frac{mA_{13e}^{[m-1]}}{A_\mu^\epsilon}\left[InA_\mu^\sigma\right] \ , \qquad N_{bI}^{[m]} = -\frac{mA_{15e}^{[m-1]}}{A_\mu^\epsilon}\left[InA_\mu^\sigma\right] \ ,$$

$$N_{nI}^{[0]} = -\frac{A_{11e}^{[0]}}{A_\mu^\epsilon}\left[InA_\mu^\sigma\right] \ , \qquad N_{nI}^{[m]} = -\frac{A_{11e}^{[m]}}{A_\mu^\epsilon}\left[InA_\mu^\sigma\right] \ ,$$

$$V_{nI}^{[m]} = -\frac{A_{15e}^{[m]}}{A_\mu^\epsilon}\left[InA_\mu^\sigma\right] \ , \qquad V_{nI}^{[0]} = -\frac{A_{15e}^{[0]}}{A_\mu^\epsilon}\left[InA_\mu^\sigma\right] \ , \tag{5.24}$$

$$V_{bT}^{[m]} = -mA_{13\alpha}^{[m-1]}(\Delta T) - mA_{33\alpha}^{[m-1]}(\Delta T) - \frac{mA_{13e}^{[m-1]}}{A_\mu^\epsilon}\left[(A_{11e\alpha} + A_{13e\alpha})(\Delta T)\right] \ ,$$

$$N_{bT}^{[m]} = -\frac{mA_{15e}^{[m-1]}}{A_{\mu}^{\epsilon}}\left[(A_{11e\alpha}+A_{13e\alpha})(\Delta T)\right] ,$$

$$N_{nT}^{[0]} = (A_{11\alpha}^{[0]}+B_{13\alpha}^{[0]})(\Delta T) - \frac{A_{11e}^{[0]}}{A_{\mu}^{\epsilon}}\left[(A_{11e\alpha}+A_{13e\alpha})(\Delta T)\right] ,$$

$$N_{nT}^{[m]} = (A_{11\alpha}^{[m]}+B_{13\alpha}^{[m]})(\Delta T) - \frac{A_{11e}^{[m]}}{A_{\mu}^{\epsilon}}\left[(A_{11e\alpha}+A_{13e\alpha})(\Delta T)\right] ,$$

$$V_{nT}^{[m]} = -\frac{A_{15e}^{[m]}}{A_{\mu}^{\epsilon}}\left[(A_{11e\alpha}+A_{13e\alpha})(\Delta T)\right] ,$$

$$V_{nT}^{[0]} = -\frac{A_{15e}^{[0]}}{A_{\mu}^{\epsilon}}\left[(A_{11e\alpha}+A_{13e\alpha})(\Delta T)\right] , \tag{5.25}$$

5.2.1 Conventional FE Matrices

Conventional finite element formulation for n^{th} order shear deformable beam with n^{th} order contraction mode is deduced from 3D FE formulation given in Section-3.2. Elements of stiffness $[K]$, coupling stiffness $[K^m]$ and mass $[M]$ matrices, are given in Appendix-C.

5.3 Spectral Finite Element Formulation of Beam

For the element formulation, the governing equations will be considered in absence of any body force, current actuation and temperature increase. We seek a time harmonic wave solution,

$$\{\mathbf{u}\} = \{u_0 \quad u_1 \quad u_2 \quad ... \quad u_{Un} \quad w_0 \quad w_1 \quad w_2 \quad ... \quad w_{Wn}\} \tag{5.26}$$

where the displacement can be written in terms of forward fourier transform as

$$\begin{aligned}\{\mathbf{u}(x,t)\} &= \sum_{n=1}^{N}\{\tilde{u_0} \quad \tilde{u_1} \quad ... \quad \tilde{u_{Un}} \quad \tilde{w_0} \quad \tilde{w_1} \quad ... \quad \tilde{w_{Wn}}\}(x)e^{-j\omega_n t} \\ &= \sum_{n=1}^{N}\{\tilde{\mathbf{u}(x)}\}e^{-j\omega_n t}\end{aligned} \tag{5.27}$$

where ω_n is the circular frequency at the n^{th} sampling point. N is the frequency index corresponding to the Nyquist frequency in the fast Fourier transform (FFT) used for computer implementation. When Equation-(5.27) is substituted into the governing equations, a set of ordinary differential equations (ODEs) is obtained for $\tilde{u_0}(x)$ and $\tilde{w_0}(x)$. Since the ODEs are of constant coefficients, the solution is of the form $\{\tilde{u_0}\}e^{-jkx}$, where k is called the wavenumber and $\{\tilde{u_0}\}$ is a vector of unknown constants. Thus, the displacement field is of the form of $\zeta e^{-j(kx+\omega t)}$, ($\zeta$ is independent of x and t), i.e., a plane wave solution is assumed. Substituting the assumed form into the set of ODEs, a matrix-vector relation is obtained:

$$[W]\{\mathbf{u}_0\} = \mathbf{0} \tag{5.28}$$

where

$$[W] = \begin{bmatrix} W_{u_0u_0} & W_{u_iu_0} & W_{w_0u_0} & W_{w_mu_0} \\ W_{u_0u_m} & W_{u_iu_m} & W_{w_0u_i} & W_{w_mu_i} \\ W_{u_0w_0} & W_{u_iw_0} & W_{w_0w_0} & W_{w_iw_0} \\ W_{u_0w_m} & W_{u_iw_m} & W_{w_0w_m} & W_{w_iw_m} \end{bmatrix} \tag{5.29}$$

where, the above matrix entries are given in Appendix-C. Since, we are interested in a nontrivial solution of $\{u_0\}$, Equation-(5.28) suggests that $[W]$ should be singular, i.e., the determinant of $[W]$ must be equal to zero. This condition gives rise to a polynomial equation in k, which must be solved as a function of ω_n. This equation is called the spectrum relation and is of the form

$$\sum_{i=0}^{2(Tn)} Q_{i+1}k^i = 0 \tag{5.30}$$

where $Tn = (2+Un+Wn)$. However, we use polynomial (quadratic) eigenvalue problem, which can solve eigenvalue problem of any order [59]. Here $[W]$ matrix is expressed as polynomial of k as

$$[W] = [P2]\ k^2 + j[P1]\ k + [P0]; \quad [P0] = \omega_n^2[P0_{AC}] + [P0_{DC}] \tag{5.31}$$

where, the above matrices are given in Appendix-C. As $[P2], [P0]$ are symmetric and $[P1]$ is anti-symmetric the roots can be written as $\pm k1, \pm k2, \pm k3...$ etc. Variation of these roots with ω_n is discussed in Section-5.4.1.3 for a particular material distribution. Once the variation of the wave numbers with frequency is known, the variation of group velocities, defined as $d\omega/d\mathbb{R}(k_i)$, can be computed numerically, where $\mathbb{R}$ denotes the real part of a complex number. The variation of the group velocities with frequency is called the dispersion relation and is an important parameter in wave propagation analysis. In the following example, we take a higher order beam and analyze it for its spectrum and dispersion relation and thereby draw several important conclusions.

5.3.1 Closed Form Solution for Cut-off Frequencies

Cut-off frequency is a frequency at which the wavenumber is zero. Since the propagating modes appear only when the loading frequency exceeds the cut-off frequency, the variation of the latter is important for the response prediction. Explicit forms of the cut-off frequencies can be obtained from the spectrum relation. Substituting $k = 0$ in the spectrum relation and solving for ω^2, the nontrivial roots can be identified. Cut-Off frequencies for FSDT and FSDT with poison contraction are given in Equation-(5.32). It is to be noted that the expression of first shear cut-off frequency is lower compare to the of first contraction mode. The expressions for both cut-off frequency is given by

$$\begin{bmatrix} 0 & 0 & \sqrt{\frac{I_0 \;\; A_{55}^{[0]}A_{11}^{\mu}+A_{15e}^{[0]\,2}}{A_{11}^{\mu}I_s}} \end{bmatrix} \qquad \begin{bmatrix} 0 & 0 & \sqrt{\frac{\left(a_{ae}-\sqrt{a_{be}}\right)I_0}{2I_sA_{11}^{\mu}}} & \sqrt{\frac{\left(a_{ae}+\sqrt{a_{be}}\right)I_0}{2I_sA_{11}^{\mu}}} \end{bmatrix} \tag{5.32}$$

where

$$\begin{aligned} I_s &= \left(I_0I_2 - {I_1}^2\right) \qquad (5.33)\\ a_{ae} &= A_{15e}^{[0]\;2} + A_{55}^{[0]}A_{11}^{\mu} + A_{33}^{[0]}A_{11}^{\mu} + A_{13e}^{[0]\;2}\\ a_{be} &= A_{15e}^{[0]\;4} + 2A_{15e}^{[0]\;2}A_{55}^{[0]}A_{11}^{\mu} - 2A_{15e}^{[0]\;2}A_{33}^{[0]}A_{11}^{\mu} + 2A_{15e}^{[0]\;2}A_{13e}^{[0]\;2} + A_{55}^{[0]2}A_{11}^{\mu\;2}\\ &\quad -2A_{55}^{[0]}A_{11}^{\mu\;2}A_{33}^{[0]} - 2A_{55}^{[0]}A_{11}^{\mu}A_{13e}^{[0]\;2} + A_{33}^{[0]2}A_{11}^{\mu\;2} + 2A_{33}^{[0]}A_{11}^{\mu}A_{13e}^{[0]\;2} + A_{13e}^{[0]\;4}. \end{aligned}$$

Note that in the absence of e_{13} and e_{15}, cut-off frequency is not dependent on coupling of the magneto-mechanical effects. For this case, the cut-off frequencies are:

$$\begin{bmatrix} 0 & 0 & \frac{I0A55}{I_s} \end{bmatrix} \qquad \begin{bmatrix} 0 & 0 & \frac{I0A55}{I_s} & \frac{I0A_{33}^{[0]}}{I_s} \end{bmatrix} \tag{5.34}$$

Cut-off frequencies for $Un = 1, Wn = 2$ are

$$\begin{bmatrix} 0 & 0 & \frac{I0A55}{I_s} & \frac{a_a+\sqrt{a_b}}{2I_a} & \frac{a_a-\sqrt{a_b}}{2I_a} \end{bmatrix} \tag{5.35}$$

Cut-off frequencies for $Un = 2, Wn = 1$ are

$$\begin{bmatrix} 0 & 0 & \frac{I_0A_{33}^{[0]}}{I_s} & \frac{b_a+\sqrt{b_b}}{2I_b} & \frac{b_a-\sqrt{b_b}}{2I_b} \end{bmatrix} \tag{5.36}$$

Cut-off frequencies for $Un = 2, Wn = 2$ are

$$\begin{bmatrix} 0 & 0 & \frac{c_a+\sqrt{c_b}}{2I_c} & \frac{c_a-\sqrt{c_b}}{2I_c} & \frac{d_a+\sqrt{d_b}}{2I_c} & \frac{d_a-\sqrt{d_b}}{2I_c} \end{bmatrix} \tag{5.37}$$

where expression for $I_s, I_a, I_b, I_c, a_a, a_b, b_a, b_b, c_a, d_a, c_b, d_b$ are given in Appendix-C. Expressions of cut-off frequencies for higher order modes and lengthy. So, numerical values of cut-off frequencies for higher order modes are discussed in Section-5.4.1.2

5.3.2 Finite Length Element

The displacement field for the two-nodded finite length element will have (Tn) forward moving and (Tn) backward moving (reflected) components. Hence, the displacement field will contain $2(Tn)$ constants. They need to be determined from $2(Tn)$ boundary conditions coming from the two nodes. The displacement at any point $x(x \in [0, L])$ and at frequency ω_n becomes

$$\{\mathbf{u}\}_n = \left\{ \begin{array}{c} \bar{u_0} \\ \bar{u_1} \\ .. \\ \bar{u_{Un}} \\ \bar{w_0} \\ \bar{w_1} \\ .. \\ \bar{w_{Wn}} \end{array} \right\} = \begin{bmatrix} R_{u_0} \\ R_{u_1} \\ .. \\ R_{u_{Un}} \\ R_{w_0} \\ R_{w_1} \\ .. \\ R_{w_{Wn}} \end{bmatrix} \begin{bmatrix} e^{-jk_1x} & 0 & .. & 0 \\ 0 & e^{-jk_2x} & .. & 0 \\ .. & .. & .. & .. \\ 0 & 0 & .. & e^{-jk_{2Tn}x} \end{bmatrix} \{a\}_n; \tag{5.38}$$

where

$$\begin{aligned} R_{u_0} &= [R_{(1)(1)} \quad R_{(1)(2)} \quad ... \quad R_{(1)(2Tn)}] \\ R_{u_1} &= [R_{(2)(1)} \quad R_{(2)(2)} \quad ... \quad R_{(2)(2Tn)}] \\ &... \\ R_{u_{Un}} &= [R_{(Un+1)(1)} \quad R_{(Un+1)(2)} \quad ... \quad R_{(Un+1)(2Tn)}] \\ R_{w_0} &= [R_{(Un+2)(1)} \quad R_{(Un+2)(2)} \quad ... \quad R_{(Un+2)(2Tn)}] \\ R_{w_1} &= [R_{(Un+3)(1)} \quad R_{(Un+3)(2)} \quad ... \quad R_{(Un+3)(2Tn)}] \\ &... \\ R_{w_{Wn}} &= [R_{(Tn)(1)} \quad R_{(Tn)(2)} \quad ... \quad R_{(Tn)(2Tn)}] \end{aligned} \tag{5.39}$$

The above equation in concise form can be written as

$$\{\mathbf{u}\}_n = [R]_n[D(x)]_n\{a\}_n, \tag{5.40}$$

where $[D(x)]_n$ is a diagonal matrix of size $[2TnX2Tn]$ whose i^{th} element is e^{jk_ix}. $[R]_n$ is the amplitude ratio matrix and is of size $[TnX2Tn]$. This matrix needs to be known beforehand for subsequent element formulation. There are several ways to compute the elements of this matrix. Before any computation, we should understand an important property of the columns of $[R]_n$ if the i^{th} column is denoted by $\{R^i\}$, then elements of $\{R^i\}$ are the coefficients of the solution corresponding to the wavenumber k_i, which amounts to saying that $R^i e^{-jk_ix}$ is a solution of the governing equation. Hence, we have the relation

$$[W(k_i)]\{R_i\}e^{-jk_ix} = 0, \quad i.e., \quad [W(k_i)]\{R_i\} = 0. \tag{5.41}$$

Equation-(5.41) is the governing equation for solving $\{R^i\}$. For nontrivial $\{R^i\}$, $[W(k_i)]$ needs to be singular, which it is if k_i is a solution of the spectrum relation. Unknown constants $\{a\}_n$ are expressed in terms of the nodal displacements by evaluating Equation-(5.40) at the two nodes, i.e. at $x = 0$ and $x = L$. In doing so, we get

$$\{u\}_n = \{u_1 \quad u_2\}_n = [T_1]_n\{a\}_n, \quad \{a\}_n = [T_1]_n^{-1}\{u\}_n. \tag{5.42}$$

where u_1 and u_2 are the nodal displacements of node 1 and node 2, respectively. Using the force boundary conditions (Equation-(5.23)), the force vector $\{f\}_n$ can be written in terms of the unknown constants $\{a\}_n$ as

$$\begin{aligned}\{f\}_n &= \{N_x^{[0]} \ldots \quad N_x^{[Un]} \quad V_x^{[0]} \ldots \quad V_x^{[Wn]}\}_n^T = [Q0]\{\mathbf{u}\}_n + [Q1]\frac{\partial\{\mathbf{u}\}_n}{\partial x} \\ &= \left([Q0][R]_n[D(x)]_n + [Q1][R]_n\frac{\partial[D(x)]_n}{\partial x}\right)\{a\}_n = [P]_n\{a\}_n\end{aligned}$$

where nonzero entries of $[Q0]$ and $Q1$ are given in Appendix-C. When the force vector is evaluated at node 1 and node 2, nodal force vectors are obtained and can be related to $\{a_n\}_n$ as

$$\{f\}_n = \{f_1 \quad f_2\}_n = [P(0) \quad P(L)]_n\{a\}_n = [T_2]_n\{a\}_n. \tag{5.43}$$

Equations-(5.42) and (5.43) together yield the relation between the nodal force and nodal displacement vector at frequency ω_n as

$$\{f\}_n = [T_2]_n[T_1]_n^{-1}\{u\}_n = [K]_n\{u\}_n. \tag{5.44}$$

where $[K]_n$ is the dynamic stiffness matrix at frequency ω_n of dimension $[2TnX2Tn]$.

5.3.3 Semi-Infinite or Throw-Off Element

Throw-off element is a one noded non-resonant beam. For the infinite length element, only the forward propagating modes are considered. The displacement field (at frequency ω_n) becomes

$$\{u\}_n = \sum_{m=1}^{Tn} R_n^m e^{-jk_{mn}x} a_m^n = [R]_n[D(x)]_n\{a\}_n, \tag{5.45}$$

where $[R]_n$ and $[D(x)]_n$ are now of size $[(Tn)\mathrm{X}(Tn)]$. $\{a\}_n$ is a vector of (Tn) unknown constants. Evaluating the above expression at node 1 ($x = 0$), nodal displacements are related to these constants through the matrix $[T_1]$ as

$$\{u_1\}_n = [R]_n[D(0)]_n\{a\}_n = [T_1]_n\{a\}_n, \tag{5.46}$$

where $[T_1]$ is now a matrix of dimension $[(Tn)\mathrm{X}(Tn)]$. Similarly, the nodal forces at node 1 can be related to the unknown constants as

$$\{f_1\}_n = [P(0)]_n\{a\}_n = [T_2]_n\{a\}_n, \tag{5.47}$$

Using Equation-(5.46) and (5.47), nodal forces at node 1 are related to the nodal displacements at node

$$\{f_1\}_n = [T_2]_n[T_1]_n^{-1}\{u\}_n = [K]_n\{u\}_n, \tag{5.48}$$

where $[K]_n$ is the element dynamic stiffness matrix of dimension $[(Tn)\mathrm{X}(Tn)]$ at frequency ω_n. It is usually complex. It is to be noted, such an element cannot be formulated in conventional finite element formulation.

5.3.4 Effect of the Temperature Field

As shown before in Equations-(5.19-5.22, 5.23), due to the temperature field both body force and nodal forces are generated. For the finite length element, the nodal force vector and body force vector due to the temperature field are

$$\begin{aligned} f^n_{nT} &= \{-N^{[0]}_{nT} \quad ... \quad -N^{[Un]}_{nT} \quad -V^{[0]}_{nT} \quad ... \quad -V^{[Wn]}_{nT} \\ &\qquad N^{[0]}_{nT} \quad ... \quad N^{[Un]}_{nT} \quad V^{[0]}_{nT} \quad ... \quad V^{[Wn]}_{nT}\}. \\ \{b_T\} &= \{N^{[0]}_{bT} \quad ... \quad N^{[Un]}_{bT} \quad V^{[0]}_{bT} \quad ... \quad V^{[Wn]}_{bT}\}. \end{aligned} \tag{5.49}$$

The equivalent nodal force due to this body force can be obtained by applying the variational principle in the frequency domain [108], which yields the load vector f^n_{bT}

$$f^n_{bT} = \int_0^L [N]^T_n\{b_T\}dx, \quad [N]_n = [R]_n[D(x)]_n[T_1]^{-1}_n, \tag{5.50}$$

where $[N]_n$ is the shape function matrix at frequency ω_n, which can be obtained by combining Equations (5.40) and (5.42).

Now integrating over the length of the element this force becomes,

$$f^n_{bT} = [R]_n[D_{-1}(x)]_n[T_1]^{-1}_n\{b_T\}. \tag{5.51}$$

where

$$[D_{-1}(x)]_n = \int_0^L [D(x)]_n dx \tag{5.52}$$

Diagonal terms of the above diagonal matrix can be written as

$$\begin{aligned} \int_0^L e^{jk_i x} dx &= \frac{e^{jk_i L} - 1}{jk_i} \quad [k_i \neq 0] \\ &= L \qquad [k_i = 0] \end{aligned} \tag{5.53}$$

5.3.5 Effect of the Actuation Current

Similar to temperature field, due to the actuation current, both body force and nodal forces are generated. For the finite length element, the nodal force vector and body force vector due to the actuation current are

$$\begin{aligned} f^n_{nI} &= \{-N^{[0]}_{nI} \quad ... \quad -N^{[Un]}_{nI} \quad -V^{[0]}_{nI} \quad ... \quad -V^{[Wn]}_{nI} \\ &\qquad N^{[0]}_{nI} \quad ... \quad N^{[Un]}_{nI} \quad V^{[0]}_{nI} \quad ... \quad V^{[Wn]}_{nI}\} \\ \{b_I\} &= \{N^{[0]}_{bI} \quad ... \quad N^{[Un]}_{bI} \quad V^{[0]}_{bI} \quad ... \quad V^{[Wn]}_{bI}\}. \end{aligned} \tag{5.54}$$

Similar to temperature field, the equivalent nodal lode due to this body force can be obtained by applying the variational principle in the frequency domain, which yields the load vector f^n_{bI}

$$f^n_{bI} = \int_0^L [N]^T_n \{b_I\} dx = [R]_n [D_{-1}(x)]_n [T_1]^{-1}_n \{b_I\}. \tag{5.55}$$

5.3.6 Solution in the Frequency Domain

The equilibrium equation at the n^{th} frequency step becomes

$$\{f\}_n - \{f\}^n_{nT} - \{f\}^n_{bT} - \{f\}^n_{nI} - \{f\}^n_{bI} = [K]_n \{u\}_n \tag{5.56}$$

This equation is solved for each frequency and nodal values of mechanical degrees freedoms are obtained. From these nodal displacements, velocities, accelerations, strains, strain rates, stresses, stress rates, magnetic fields, magnetic flux densities and sensor open circuit voltages can be calculated for each frequency in following manner:

5.3.6.1 Strain Computation

The expressions of strain can be found using Equations-(5.40) and (5.42) for the finite length element and similar expressions for the infinite length element. Using Equation

(5.3) along with the previous equations, the strains at a point (x, z) of an element can be related to the nodal displacements of that element as

$$
\begin{aligned}
\varepsilon_{xx}^{-} &= \left[[R_{u_0}] + \sum_{i=1}^{Un} z^i [R_{u_i}]\right] [D_1(x)]_n \{a\}_n - \alpha(\Delta T), \\
\varepsilon_{zz}^{-} &= \left[\sum_{i=1}^{Wn} i z^{i-1} [R_{w_i}]\right] [D(x)]_n \{a\}_n - \alpha(\Delta T), \\
\varepsilon_{xz}^{-} &= \left[\left(\sum_{i=1}^{Un} i z^{i-1} [R_{u_i}]\right) [D(x)]_n + \left([R_{w_0}] + \sum_{i=1}^{Wn} z^i [R_{w_i}]\right) [D_1(x)]_n\right] \{a\}_n,
\end{aligned}
\tag{5.57}
$$

where

$$
[D_1(x)]_n = \frac{\partial}{\partial x} [D(x)]_n.
$$

In matrix form, the above equations can be written as

$$
\{\varepsilon\} = \left([B_0][D(x)] + [B_1][D_1(x)]\right) [T_1]^{-1} \{u\} - \{\varepsilon\}_T, \tag{5.58}
$$

where

$$
[B_0] = \begin{bmatrix} 0 \\ \sum_{i=1}^{Wn} i z^{i-1} [R_{w_i}] \\ \sum_{i=1}^{Un} i z^{i-1} [R_{u_i}] \end{bmatrix}, \quad [B_1] = \begin{bmatrix} [R_{u_0}] + \sum_{i=1}^{Un} z^i [R_{u_i}] \\ 0 \\ [R_{w_0}] + \sum_{i=1}^{Wn} z^i [R_{w_i}] \end{bmatrix}. \tag{5.59}
$$

where $\{\varepsilon\}_T$ is the strain due to temperature whose elements are $\alpha(\Delta T)\{1\ 1\ 0\}$. It is to be noted that the above expressions are to be evaluated at each frequency ω_n.

5.3.6.2 Magnetic Field Calculation.

Magnetic field can be calculated from Equation-(5.17) as

$$
\bar{H} = -\frac{1}{A_\mu^\epsilon} \left([[B_{H0}][D(x)] + [B_{H1}][D_1(x)]] [T_1]^{-1} \{u\} - \{H\}_I - \{H\}_T \right), \tag{5.60}
$$

where

$$
\begin{aligned}
&[B_{H0}] = \sum_{i=1}^{Wn} i A_{13e}^{[i-1]} [R_{w_i}] + \sum_{i=1}^{Un} i A_{15e}^{[i-1]} [R_{u_i}], \\
&[B_{H1}] = A_{11e}^{[0]} [R_{u_0}] + \sum_{i=1}^{Un} A_{11e}^{[i]} [R_{u_i}] + A_{15e}^{[0]} [R_{w_0}] + \sum_{i=1}^{Wn} A_{15e}^{[i]} [R_{w_i}] \\
&[H_I] = -In A_\mu^\sigma, \qquad [H_T] = -(A_{11e\alpha} + A_{13e\alpha})(\Delta T)
\end{aligned}
$$

5.3.6.3 Stress and Magnetic Flux Density Calculation.

The constitutive relationship given in Equation-(2.9) can now be used to compute the stresses and magnetic flux density.

$$\{\bar{\sigma}\} = [Q]\{\bar{\epsilon}\} - [e]^T\{\bar{H}\} = \left([\sigma_0][D(x)] + [\sigma_1][D_1(x)]\right)[T_1]^{-1}\{u\} + \{\sigma\}_T + \{\sigma\}_I, \quad (5.61)$$

$$\{\bar{B}\} = [e]\{\bar{\epsilon}\} + [\mu^\epsilon]\{\bar{H}\} = \left([B_0][D(x)] + [B_1][D_1(x)]\right)[T_1]^{-1}\{u\} + \{B\}_T + \{B\}_I, \quad (5.62)$$

where

$$\begin{aligned}
&[\sigma_0] = [Q][B_0] + \frac{1}{A_\mu^\epsilon}[e]^T[B_{H0}], \quad [\sigma_1] = [Q][B_1] + \frac{1}{A_\mu^\epsilon}[e]^T[B_{H1}],\\
&[\sigma_I] = -\frac{1}{A_\mu^\epsilon}[e]^T\{H\}_I, \quad [\sigma_T] = -[Q]\{\epsilon\}_T - \frac{1}{A_\mu^\epsilon}[e]^T\{H\}_T.\\
&[B_0] = [e][B_0] - \frac{1}{A_\mu^\epsilon}[\mu^\epsilon][B_{H0}], \quad [B_1] = [e][B_1] - \frac{1}{A_\mu^\epsilon}[\mu^\epsilon][B_{H1}],\\
&[B_I] = \frac{1}{A_\mu^\epsilon}[\mu^\epsilon]\{H\}_I, \quad [B_T] = -[e]\{\epsilon\}_T + \frac{1}{A_\mu^\epsilon}[\mu^\epsilon]\{H\}_T.
\end{aligned}$$

It is to be noted that the above expressions are to be evaluated at each frequency ω_n.

5.3.6.4 Computation of Sensor Open Circuit Voltage.

The open circuit voltage in the sensor for each frequency can be calculated from Equation-(3.33) as:

$$\begin{aligned}
\bar{V} &= n_s\{l_c\}^T \int_v \frac{\partial}{\partial t}\{\mu^\sigma \bar{H}\}dv \quad (5.63)\\
&= \frac{n_s A_p}{A_\mu^\epsilon}(j\omega_n)[\mu^\sigma]\left([B_{H0}][D_{-1}(x)] + [B_{H1}][D(x)]\right)[T_1]^{-1}\{u\}
\end{aligned}$$

where A_p is cross sectional area of the magnetostrictive patch p.

5.3.6.5 Time Derivatives of any Variable.

Time derivatives of any variable can be expressed by multiplying with $-j\omega_n$ with the variable in the corresponding frequency. Hence, velocity and acceleration for each frequency can be obtained from displacement as

$$\{\dot{u}\}_n = -j\omega_n\{u\}_n \qquad \{\ddot{u}\}_n = (-j\omega_n)^2\{u\}_n \quad (5.64)$$

Table 5.1: First 10 natural frequencies for 0_{10} and $0_5/90_5$ layup using 2D FEM

0_{10}	337	1938	4853	5316	8382	12239	15985	16202	20270	24300
$0_5/90_5$	157	948	2502	3856	4582	6897	9375	11278	12077	14220

5.4 Numerical Results and Discussion

In this section, numerical experiments are performed to get sensor response history from the mechanical loading and vice versa in spectral domain. First, the different orders of elements are used to model a composite cantilever beam subjected to tip vertical load (shown in Figure-4.1), and the response histories are compared to show the need for higher order spectral elements for high frequency loading. Next, the formulated spectral element is used for reconstruction of impact force from sensor response histories of the structure, which is also called force identification problem. For numerical computation, total thickness of the laminate is considered as 50mm in ten layers. Different types of layup sequences ($[0_{10}], [0_5/90_5], [m/0_4/90_4/m]$) are considered for numerical analysis. Where m stands for magnetostrictive layer. Length of the beam is considered as 0.5m. For lay up of $[0_{10}]$, 10 unidirectional layup is considered of each 5mm thick. In $[m/0_4/90_4/m]$ layup sequence, top and bottom layers are made up of magnetostrictive materials each of 5mm thick. In between, there are eight composite layer of total 40mm thickness with top 4 layers of 0 degree and bottom 4 layers of 90 degree ply sequences. The material properties of magnetostrictive materials are assumed as $E = 30$GPa, $\varrho = 9250$kg/m^3, while those of composite are $E_1 = 180$GPa, $E_2 = 10.3$GPa, $G_{12} = 28$GPa and $\varrho = 1600$kg/m^3, respectively.

5.4.1 Free Vibration and Wave Response Analysis

Various studies are performed to demonstrate the requirement of higher order elements for high frequency loading. First, free vibration study is performed to show the errors in first 10 natural frequencies of the cantilever beam with different beam theory assumptions. Then, cut off frequencies, spectrum relations and dispersion relations of the beam are discussed in the context of different beam theory assumptions. Finally, responses for modulated and impulse forces are studied using the formulated spectral elements.

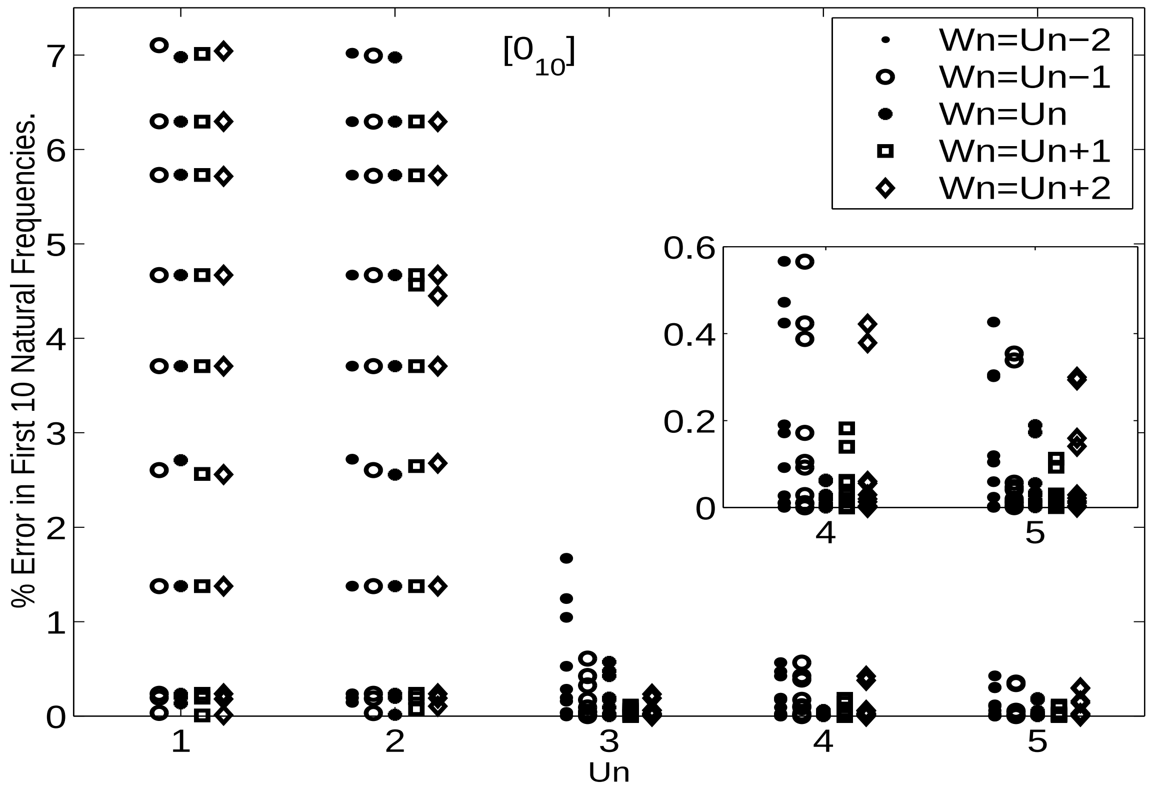

(a) 0_{10} Layup

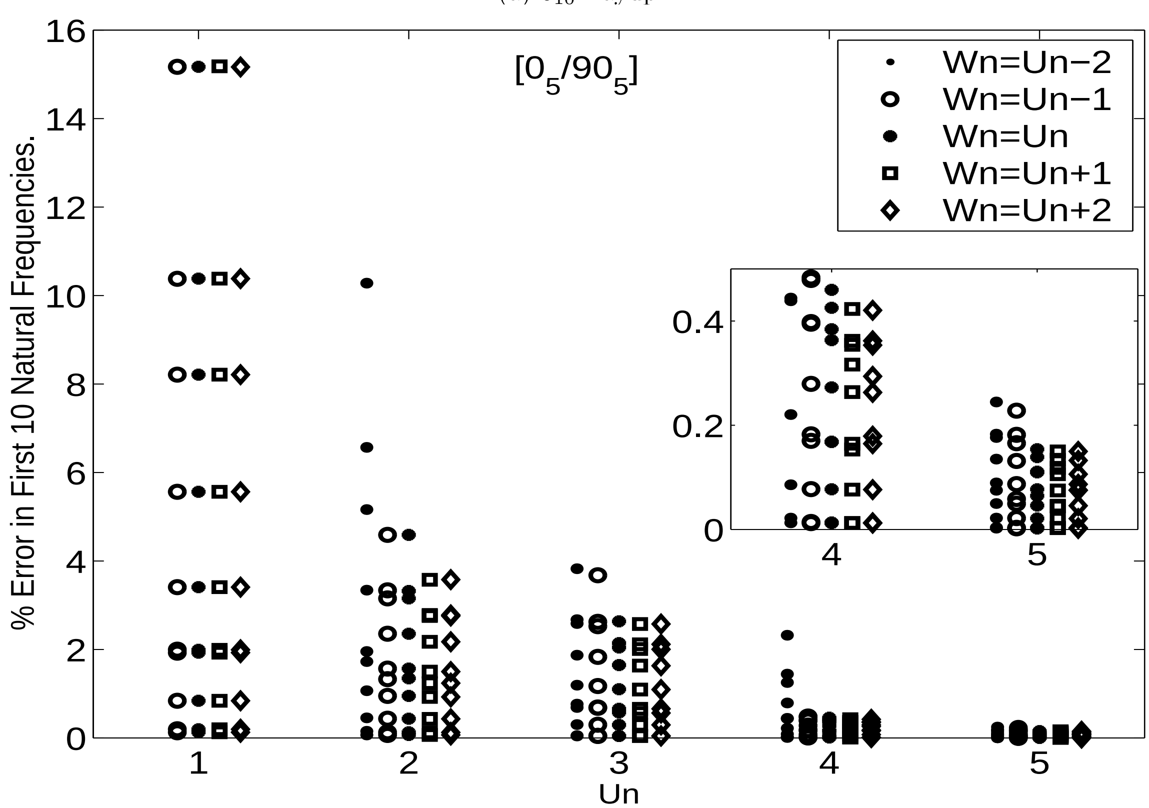

(b) $0_5/90_5$ Layup

Figure 5.1: Error in Natural Frequency for Different Beam Assumptions

5.4.1.1 Free Vibration Study

Percentage errors of first 10 natural frequencies with different beam theory assumptions are studied for a symmetric ($[0_{10}]$) and an asymmetric ($[0_5/90_5]$) layup sequence and shown in Figure-5.1, where stiffness and mass matrices are taken from Section-5.2.1. Zoomed results for $Un = 4$ and 5 are also shown in the inset of the figures. Frequencies obtained from 2D analysis is taken as baseline and shown in Table-5.1. FE analysis is performed with 500X40 numbers of 2D plane strain elements. For symmetric layup sequence ($[0_{10}]$), results with first ($Un = 1$) and second ($Un = 2$) order, and for third ($Un = 3$) and fourth ($Un = 4$) order shear deformable assumption gives similar results. Similarly for asymmetric layup sequence ($[0_5/90_5]$), results with second ($Un = 2$) and third ($Un = 3$) order and fourth ($Un = 4$) and fifth ($Un = 5$) order shear deformable assumption gives similar results.

For $[0_{10}]$ layup sequence (Figure-5.1(a)), first ($Un = 1$) and second ($Un = 2$) order shear deformable assumptions give 7% error. Third order ($Un = 3$) shear deformable beam with one contraction mode ($Wn = 1$) gives 1.8% error. However, with the inclusion of two or more contraction modes gives results that have 0.5% error. For $[0_5/90_5]$ layup sequence (Figure-5.1(b)), first order ($Un = 1$) shear deformable assumptions give 15% error, which is quite high. Second order shear deformable beam ($Un = 2$) with one contraction mode ($Wn = 1$) gives 10% error. Second ($Un = 2$) and third ($Un = 3$) order shear deformable beam with two or more contraction modes ($Wn > 1$) gives results that has 5% error. Fourth order shear deformable beam ($Un = 4$) with second order contraction mode ($Wn = 2$) shows 2.5% error. Fourth and fifth order shear deformable beam with higher order contraction shows 0.4% and 0.2% error respectively (inset of the figure). This study clearly demonstrates the need for higher order theories for accurate response estimation.

5.4.1.2 Cut-Off Frequencies of Beam.

In this example, the wavenumber variations are plotted for different orders. Closed form solution of the cut-off frequencies for FSDT and FSDT with contraction effect beam theories is given in Section-5.3.1. These closed form solutions for higher order theories are lengthy. Hence, the numerically obtained values are used in these studies. Figure-5.2 and Figure-5.3 show the cut-off frequencies for fifth order shear deformable ($Un = 5$) beam with varying contraction mode and fifth order contraction mode ($Wn = 5$) with varying shear deformable beam assumptions. Figure-5.2(a) and Figure-5.3(a) show the cut-off

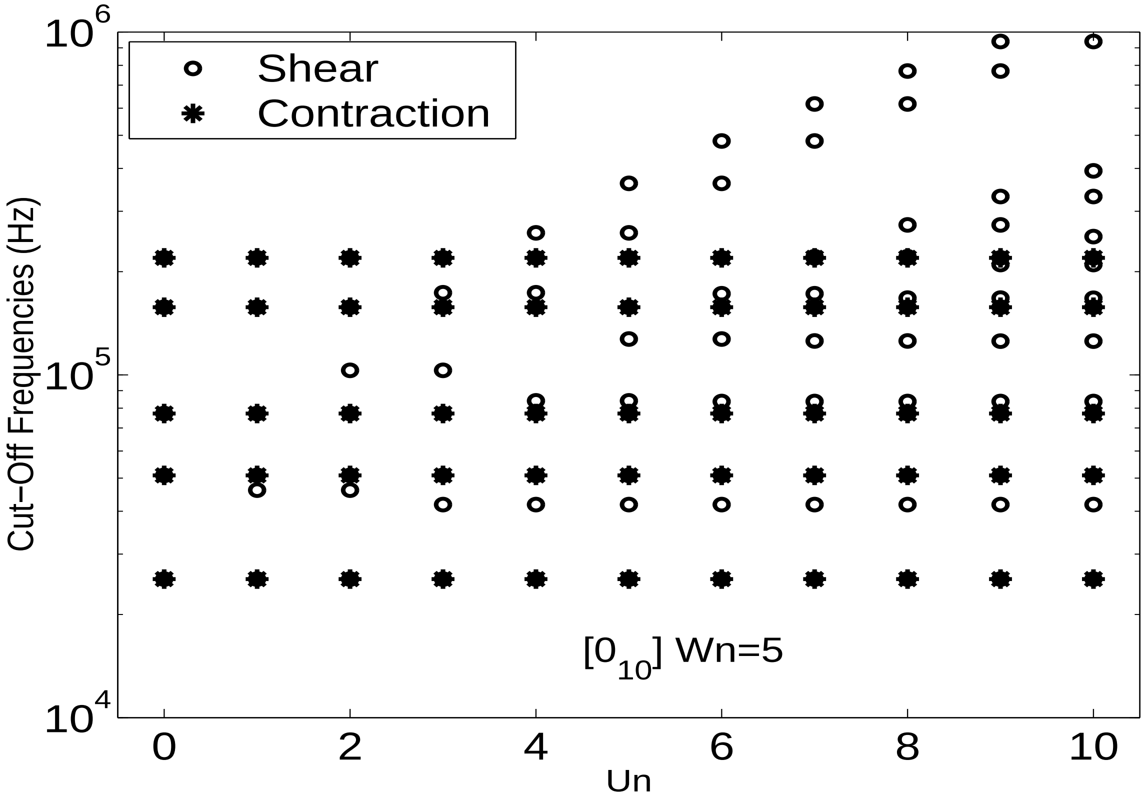

(a) $Wn = 5$

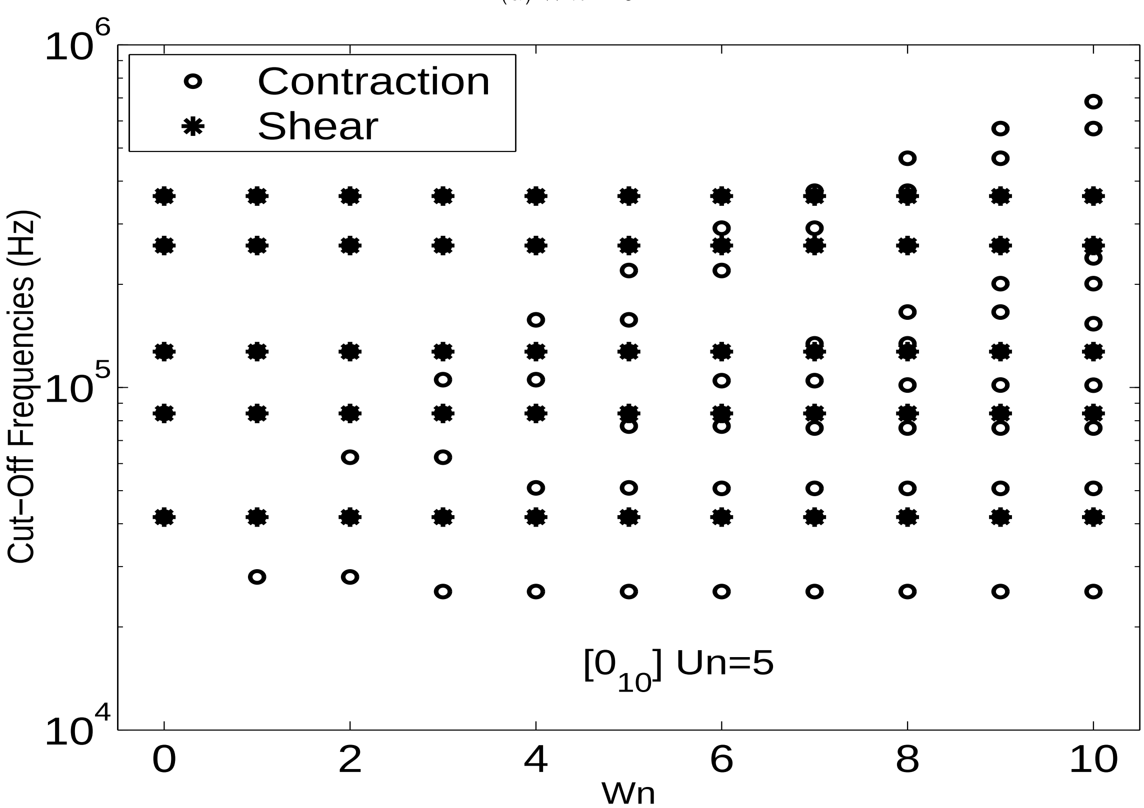

(b) $Un = 5$

Figure 5.2: Cut-Off Frequencies for $[0_{10}]$ Layup with different beam assumptions.

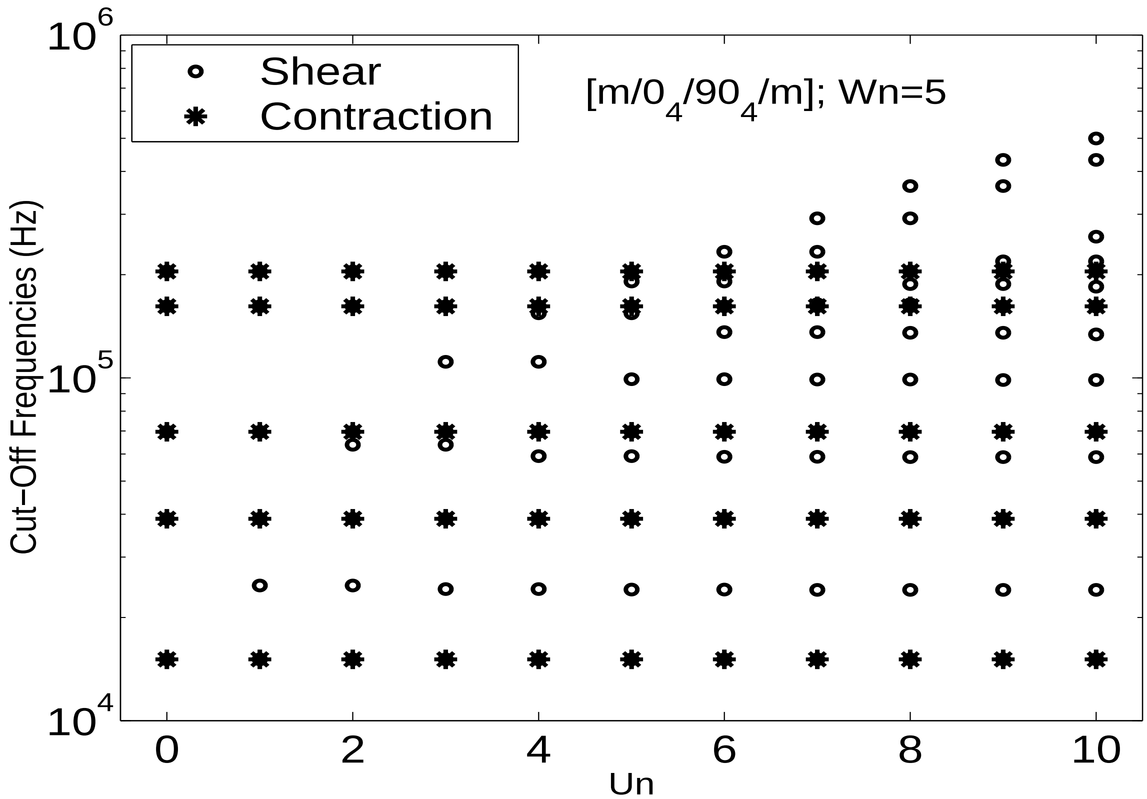

(a) $Wn = 5$

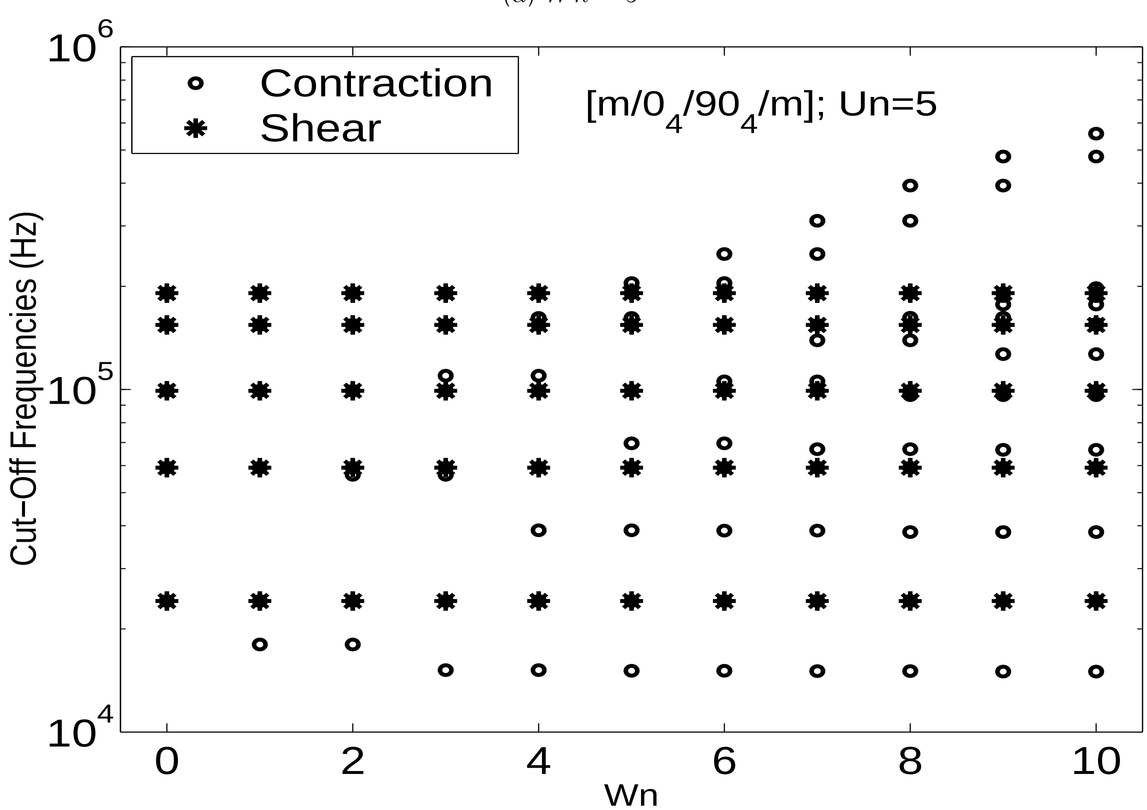

(b) $Un = 5$

Figure 5.3: Cut-Off Frequencies for $[m/0_4/90_4/m]$ layup with different beam assumptions.

frequencies for the $[0_{10}]$ and $[m/0_4/90_4/m]$ lay up sequences respectively. For both the cases, we have five contraction cut-off frequencies and 0 to 10 numbers of shear cut-off frequencies depending upon the beam theory assumption. Observations from these figures are as follows:

- The figure shows that first contraction cut-off frequency is below the first shear cut-off frequency. It shows the importance of consideration of contraction mode in the analysis.

- If the loading frequency is 100kHz (say), at least three contraction modes with three shear modes for $[m/0_4/90_4/m]$ lay up sequence and three contraction modes with two shear modes for $[0_{10}]$ lay up sequence should be considered in the dynamic analysis. Classical beam theory is sufficient for $[0_{10}]$ and $[m/0_4/90_4/m]$ layup sequences up to loading frequency of 20, and 10 kHz respectively.

- Contraction mode cut off frequencies are nearly constant irrespective of assumption on the shear deformation.

- Shear cut-off frequencies follow a particular pattern when the order of shear deformation assumption is two more than the corresponding shear mode. For example, first shear cut-off frequency is same for $Un = 1$ and $Un = 2$. For $Un = 3$, this value is little less than previous. This value is again constant for $Un = 3$ and onwards.

Figure-5.2(b) and Figure-5.3(b) shows the cut-off frequencies for $[0_{10}]$ and $[m/0_4/90_4/m]$ lay up sequences considering $Un = 5$ and varying Wn from 0 to 10 respectively. For both the cases we have five shear cut-off frequencies and 0 to 10 numbers of contraction cut-off frequencies depending upon the assumption. Observations from these figures are as follows:

- Figure shows that the first contraction cut-off frequency is below the first shear cut-off frequency. Again, it shows the importance of inclusion of lateral contractions in the analysis.

- If the loading frequency is 100kHz (say), at least three contraction modes with three shear modes for $[m/0_4/90_4/m]$ lay up sequence and three contraction modes with two shear modes for $[0_{10}]$ lay up sequence should be considered in the dynamic analysis. Classical beam theory is sufficient for $[0_{10}]$ and $[m/0_4/90_4/m]$ layup sequences up to loading frequency of 20, and 10 kHz respectively.

- Shear mode cut off frequencies are always constant irrespective of assumption on the order of contraction.

- Contraction mode cut-off frequencies follow a particular pattern when the order of contraction assumption is two more than the corresponding contraction mode. For example, first contraction cut-off frequency is same for $Wn = 1$ and $Wn = 2$. For for $Wn = 3$, this value is little less than previous. This value is again constant for $Wn = 3$ and onwards.

5.4.1.3 The Spectrum and Dispersion Relation

Spectrum and Dispersion relation indicate the nature of waves that is, dispersive or non-dispersive. These relations are derived independent of the boundary condition of the structure. However, they depend on the material properties. If the loading is "monochromatic" (i.e., it contains a single frequency), the dispersion relation can be used to predict the response especially for highly dispersive waves. Axial, bending, shear and contraction wavenumbers, can be identified from the dispersion relationships. The wavenumbers plotted in the negative side of the ordinate denote the imaginary part of the wavenumbers (damping mode)[59, 60, 61, 62, 63, 64]. The frequencies where the imaginary wavenumbers become real are called the cut-off frequencies. It is important to note that there are propagating axial and bending modes for all frequencies, whereas the shear and contraction mode appear only when the frequency exceeds the respective cut-off frequencies.

Figure-5.4 and Figure-5.5 show the spectrum relationships and group speeds for $[0_{10}]$ layup sequences with different beam theory assumptions. Figure-5.4(a) shows the spectrum relationships for fourth order shear deformable beam assumption with first order contraction mode ($Un = 4, Wn = 1$). Hence, four shear cut-off frequencies and one contraction cut-off frequency are shown in the figure. Figure-5.4(c) shows the spectrum relationships for $Un = 1, Wn = 4$. Hence, one shear cut-off frequency and four contraction cut-off frequencies are seen in the figure. Figure-5.4(e) shows the spectrum relationships for fourth order shear deformable beam assumption with fourth order contraction mode ($Un = 4, Wn = 4$). Hence, four shear cut-off frequencies and four contraction cut-off frequencies are seen in the figure. Following behavior can be observed from these figures:

- At high frequency, all contraction modes are going near to bending mode and all shear modes are going to near of axial mode.

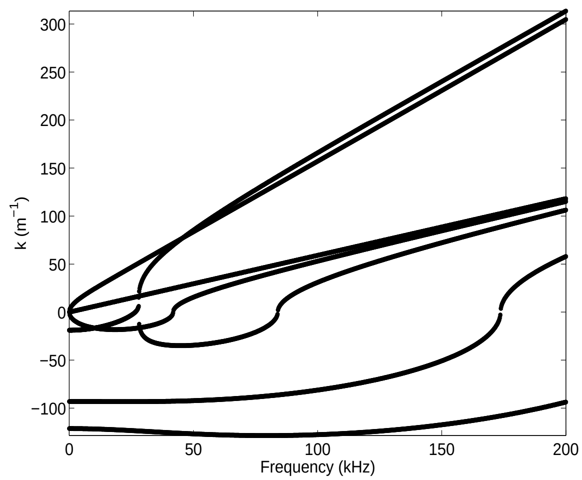

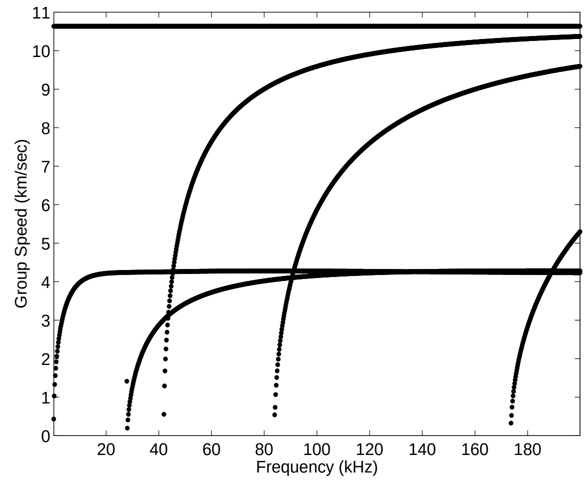

(a) Spectrum $Un = 4, Wn = 1$

(b) Group Speed $Un = 4, Wn = 1$

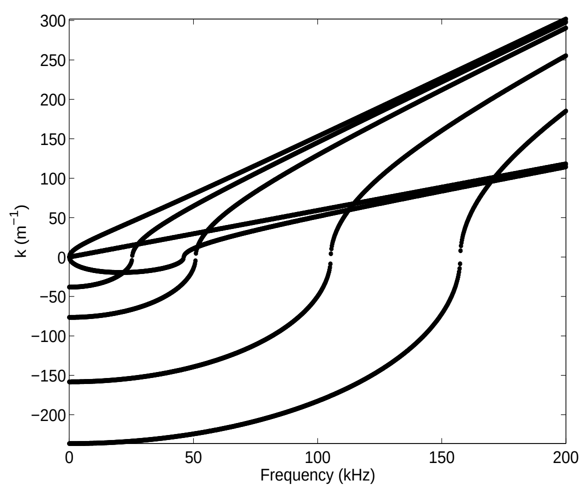

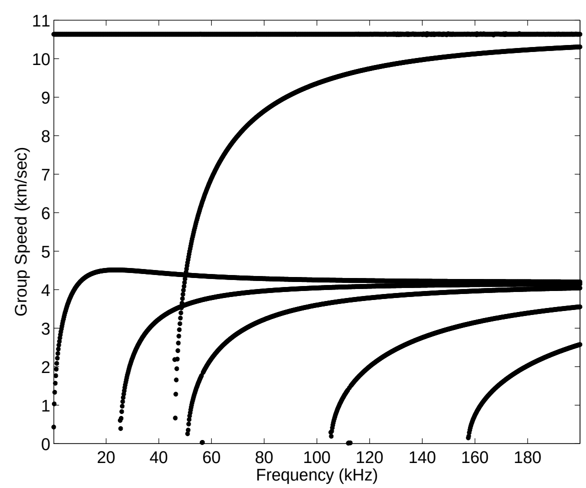

(c) Spectrum $Un = 1, Wn = 4$

(d) Group Speed $Un = 1, Wn = 4$

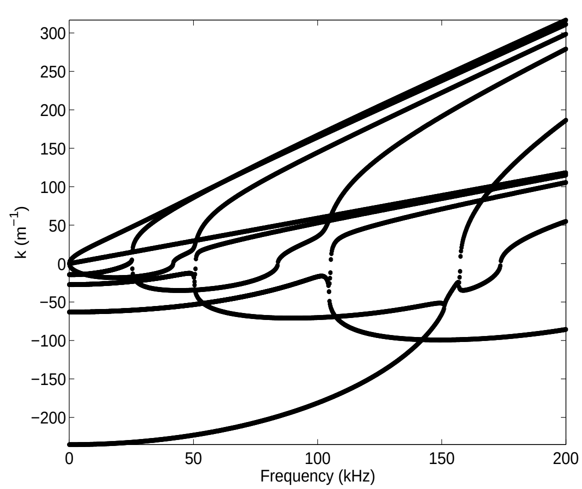

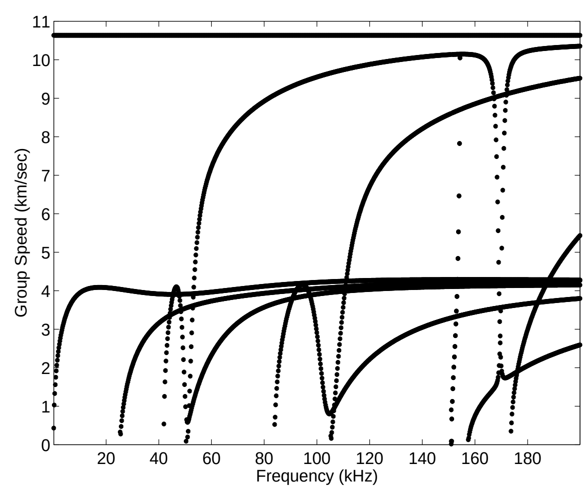

(e) Spectrum $Un = 4, Wn = 4$

(f) Group Speed $Un = 4, Wn = 4$

Figure 5.4: Spectrum Relationships and Group Speeds for $[0_{10}]$.